Closed expressions for partial-wave photoelectron spectra and angular distributions: A ground-state hydrogen atom struck by a temporal δ-function pulse

K. G. Kim, C. C. Widmayer, and M. D. Girardeau
Department of Physics, Chemical Physics Institute and Institute of Theoretical Science, University of Oregon, Eugene, Oregon 97403
(Received 5 November 1992)

A method of dealing with hypergeometric functions to obtain closed expressions for partial-wave components of photoelectron spectra in terms of elementary functions is presented through an example of a hydrogen atom struck by a temporal δ-function pulse. Based on this method, angular distributions of photoelectrons with various energies are presented for a wide range of field strengths from a perturbative (field strength ~ 0.05 a.u., 1 a.u. $= 5.14 \times 10^9$ V/cm) to a superintense regime (field strength ~ 5 a.u.).

PACS number(s): 32.80.Fb, 32.80.Rm, 42.50.Hz

I. INTRODUCTION

Owing to the rapid development of laser techniques, very intense fields of strength comparable to that of the atomic field can be provided to investigate atomic response to strong radiation, especially photoionization. Since the observation of the phenomenon of so-called above-threshold ionization (ATI) by Agostini *et al.* [1], much work, both theoretical and experimental, has been done on this strong-field area, leading to the discovery and prediction of novel effects such as peak suppression [2,3], subpeak structure within a single ATI peak [4,5], high-order harmonic generation [6,7], and stabilization against ionization [8,9] under superstrong fields.

It is well known that one can obtain pure atomic response (photoelectron spectra) experimentally by using a short-pulse laser (on the order of femtoseconds, preferably) rather than a long, monochromatic one, since in the former case one can minimize the effect of final-state scattering inside the focusing region, the so-called ponderomotive scattering, on photoelectron spectra. However, due to the finite temporal profiles of pulses and their significant effects on the above-mentioned phenomena, especially those of turning on and off of pulses [10], one does not expect a purely analytic explanation or prediction for such phenomena by finding the exact time evolution of electronic wave functions under both atomic and laser fields. Thus, one of the most popular methods in this strong-field area, which takes into account the influence of the envelope function for the temporal variation of the laser intensity, is a direct numerical integration of the time-dependent Schrödinger equation (TDSE), usually employing some technique such as the Kramers-Henneberger transformation [11] at the early stage of calculations.

On the other hand, in our previous paper [12], we developed a useful representation called "impulse representation" for obtaining the time evolution of a single-electron wave function of an atom subjected to intense, ultrashort laser pulses. Although we expect that numerical calculation will be required at some stage of the calculations for a realistic laser pulse, we demonstrated there the effectiveness of the representation especially for ultrashort pulses by obtaining exact results for survival, excitation, and ionization probabilities, and photoelectron spectra of the ground-state hydrogen atom struck by a temporal δ-function pulse. In this paper, we present closed expressions for partial-wave components of photoelectron spectra in that case with a demonstration of some techniques to deal with the relevant hypergeometric functions. After a few fundamental remarks on the derivation of the "doubly differential cross section" (DDCS, see the content for its definition) in Sec. III, we show the angular distributions of photoelectrons generated for various field strengths (0.05–5 a.u.) with tables of relevant data in Sec. IV. We would like to point out the fact that many authors have recently reported measurements or calculations [13,14] of angular distributions for photoelectrons since the comparison of theoretical calculation to experimental data can provide one of the good bases for testing the validity of a theory.

The techniques in Sec. II can reduce computational times as compared to the direct use of any package which recognizes hypergeometric functions, and further, we believe they can be extended to other problems related to nonrelativistic hydrogenic wave functions in connection with optical processes, e.g., explicit evaluations of dipole or multipole matrix elements, especially for continuum-continuum transitions [15]. Although the δ-function pulse is not realistic in the sense that it contains the entire range of frequencies with equal amplitudes, the data we present can shed light on the understanding of atomic response as laser-pulse intensity changes from a very perturbative value to a superatomic one.

II. METHODS OF OBTAINING CLOSED EXPRESSIONS FOR PARTIAL-WAVE COMPONENTS OF PHOTOELECTRON SPECTRA

Although the following procedure is applicable to any initial state of a nonrelativistic Coulombic system, we will confine ourselves here to the case of a hydrogen atom initially prepared in the ground state $\Psi_{100}(\mathbf{r})$, struck by a δ-function pulse $\mathbf{E}(t)=\mathbf{F}\delta(t)$ for the sake of concrete

demonstration of the procedure. According to the formalism developed previously [12], the wave function in momentum space right after the pulse at time $t=0^+$ is given by

$$\Phi(\mathbf{p},0^+)=\Phi_{100}(\mathbf{p}+\mathbf{F}) , \tag{1}$$

where Φ_{100} is the ground-state wave function in momentum space. In coordinate space,

$$\begin{aligned}\Psi(\mathbf{r},0^+)&=(2\pi)^{-3/2}\int d^3p\, e^{-i\mathbf{p}\cdot\mathbf{r}}\Phi(\mathbf{p},0^+)\\&=e^{-i\mathbf{F}\cdot\mathbf{r}}(2\pi)^{-3/2}\int d^3p' e^{i\mathbf{p}'\cdot\mathbf{r}}\Phi_{100}(\mathbf{p}')\\&=e^{-i\mathbf{F}\cdot\mathbf{r}}\Psi_{100}(\mathbf{r}) .\end{aligned} \tag{2}$$

The transition amplitude C_{klm} to a continuum state specified by a set of quantum numbers (k,l,m) is given by

$$C_{klm}=\int d^3r\, \Psi^*_{klm}(\mathbf{r})\Psi(\mathbf{r},0^+) . \tag{3}$$

Using the formula for partial-wave expansion of the plane wave $e^{-i\mathbf{F}\cdot\mathbf{r}}$

$$e^{-i\mathbf{F}\cdot\mathbf{r}}=\sum_{l=0}^{\infty}(-i)^l(2l+1)j_l(Fr)P_l(\cos\theta) , \tag{4}$$

and the continuum wave function of the form [16]

$$\Psi_{klm}(\mathbf{r})=R_{kl}(r)Y_{lm}(\theta,\phi) , \tag{5}$$

with

$$\begin{aligned}R_{kl}=&C_k^{(l)}\frac{(2kr)^l}{(2l+1)!}\\&\times e^{-ikr}{}_1F_1(ik^{-1}+l+1;2l+2;2ikr) ,\end{aligned} \tag{6}$$

one can easily perform the angular part of the integration (3). Here j_l and P_l are, respectively, the spherical Bessel function and the Legendre polynomial, and ${}_1F_1(\alpha;\beta;\chi)$ and $C_k^{(l)}$ are, respectively, the confluent hypergeometric function and the k-normalization factor for continuum states, which are given as

$$\begin{aligned}{}_1F_1(\alpha;\beta;\chi)&=\sum_{n=0}^{\infty}\frac{\Gamma(\alpha+n)\Gamma(\beta)}{\Gamma(\alpha)\Gamma(\beta+n)}\frac{\chi^n}{n!}\\&=1+\frac{\alpha}{\beta}\frac{\chi^1}{1!}+\frac{\alpha(\alpha+1)}{\beta(\beta+1)}\frac{\chi^2}{2!}+\cdots\end{aligned} \tag{7}$$

and

$$C_k^{(l)}=\left[\frac{4k}{1-e^{-2\pi/k}}\right]^{1/2}\prod_{s=1}^{l}\left[\frac{1+s^2k^2}{k^2}\right]^{1/2} . \tag{8}$$

Then we have

$$\begin{aligned}C_{klm}=C_{kl0}\delta_{m,0}=\delta_{m,0}(-1)^l2^{l+1}&\frac{(2l+1)^{1/2}}{(2l+1)!}C_k^{(l)}k^l\\&\times\int dr\, r^{l+2}e^{-(1-ik)r}j_l(Fr)\,{}_1F_1(-ik^{-1}+l+1;2l+2;-2ikr) .\end{aligned} \tag{9}$$

It should be noted that we have chosen to change representation from momentum space to coordinate space in order to facilitate the evaluation of the integral in Eq. (9). The coordinate-space bound state wave function includes the factor $e^{-r/n}$, which assures rapid convergence [17] of integration. Several steps of calculation with the aid of the integral table [18] yield the following expression for C_{kl0}:

$$\begin{aligned}C_{kl0}&=-iC_k^{(l)}\frac{(2l+1)^{1/2}}{(2l+1)!}(2k)^lF^{-1}[(-1)^lZ_l-Z_l^*]\\&=C_k^{(l)}\frac{(2l+1)^{1/2}}{(2l+1)!}2^{l+1}k^lF^{-1}\\&\quad\times\begin{cases}\mathrm{Im}(Z_l) & \text{for even } l\\ i\,\mathrm{Re}(Z_l) & \text{for odd } l ,\end{cases}\end{aligned} \tag{10}$$

where

$$\begin{aligned}Z_l=&z_2^{-(l+2)}\\&\times\sum_{n=0}^{l}\frac{(l+n)!(l-n+1)}{n!}\left[\frac{iz_2}{2F}\right]^n\\&\times{}_2F_1(ik+l+1,l-n+2;2l+2;2ikz_2^{-1}) ,\end{aligned} \tag{11}$$

with $z_2=1+i(k-F)$ and ${}_2F_1(\alpha,\beta;\gamma;\chi)$ being the ordinary hypergeometric function.

The expression (10) is sufficient to perform numerical evaluations of photoelectron spectra using a commercial mathematical package such as MATHEMATICA, but it would be preferable to express it in terms of elementary functions rather than the summation over hypergeometric functions. In order to do this, we can use the following properties of hypergeometric functions including a recursion relation and differential equation [19], which relate hypergeometric functions of different arguments:

$${}_2F_1(\alpha,\beta;\gamma;\chi)=1 \text{ if one of } \alpha \text{ and } \beta \text{ is zero} , \tag{12}$$

$${}_2F_1(\alpha,\beta;\gamma;\chi)={}_2F_1(\beta,\alpha;\gamma;\chi) , \tag{13}$$

$${}_2F_1(\alpha,\beta;\beta;\chi)=(1-\chi)^{-\alpha} , \quad \chi\neq 1 , \tag{14}$$

$${}_2F_1(\alpha,\beta;\gamma;0)=1 , \tag{15}$$

$$\begin{aligned}&[2\beta-\gamma+(\alpha-\beta)\chi]\,{}_2F_1(\alpha,\beta;\gamma;\chi)\\&\quad+(\gamma-\beta)\,{}_2F_1(\alpha,\beta-1;\gamma;\chi)\\&\quad+\beta(\chi-1)\,{}_2F_1(\alpha,\beta+1;\gamma;\chi)=0 ,\end{aligned} \tag{16}$$

$$\frac{d^n}{d\chi^n}[(1-\chi)^{\alpha+\beta-\gamma}{}_2F_1(\alpha,\beta;\gamma;\chi)] = \frac{(\gamma-\alpha)_n(\gamma-\beta)_n}{(\gamma)_n}(1-\chi)^{\alpha+\beta-\gamma-n}{}_2F_1(\alpha,\beta;\gamma+n;\chi) , \tag{17}$$

$${}_2F_1(\alpha,1;2;\chi)=(\alpha-1)^{-1}\chi^{-1}[(1-\chi)^{-(\alpha-1)}-1] , \tag{18}$$

where

$$(C)_n=\begin{cases}1 & \text{if } n=0\\ C(C+1)\cdots(C+n-1) & \text{otherwise .}\end{cases} \tag{19}$$

Here Eq. (18) is derived from Eq. (16) by setting $\beta=1$ and $\gamma=2$ with help of Eqs. (12) and (14). In our present case, we need an expression for ${}_2F_1(\alpha,1;2l+2;\chi)$ with $\alpha=ik^{-1}+l+1$ and $\chi=2ikz_2^{-1}$, which can be derived from Eqs. (17) and (18) as

$$\begin{aligned}{}_2F_1(ik^{-1}+l+1,1;2l+2;2ikz_2^{-1}) &= -2^{-(2l+1)}\frac{(2l+1)!}{\prod_{s=0}^{l}(1+s^2k^2)}z_2^{2l+1}\\ &\times\left\{\left[\frac{z_1}{z_2}\right]^{l-ik^{-1}}-\sum_{m=0}^{2l}\frac{(ik^{-1}-l)_m}{m!}\left[\frac{2ik}{z_2}\right]^m\right\},\end{aligned} \tag{20}$$

where $z_1=1-i(k+F)$. In this case the recursion relation of Eq. (16) becomes

$${}_2F_1(ik^{-1}+l+1,l-n+2;2l+2;2ikz_2^{-1})=-\frac{2(n+1-inF)}{(l-n+1)z_1}{}_2F_1(ik^{-1}+l+1,l-n+1;2l+2;2ikz_2^{-1}) + \frac{(l+n+1)z_2}{(l-n+1)z_1}{}_2F_1(ik^{-1}+l+1,l-n;2l+2;2ikz_2^{-1}) . \tag{21}$$

Now we can express the finite sum of Eq. (11) over the running variable n in terms of two hypergeometric functions having values of the second argument β equal to 0 and 1, whose explicit expressions are known from Eqs. (12) and (20). Although it is not necessary in obtaining a final form of the expression, one can easily show that the quantities relevant to the final result are the first term in the curly bracket of Eq. (20) and its overall coefficient to be obtained after the reduction mentioned above. The reason for this is that the terms other than those, upon reduction, become pure real (imaginary), while we need only the imaginary (real) part of Z_l for obtaining C_{kl0} [see the second expression for C_{kl0} in Eq. (10)]. This fact can save much computational time, especially in symbolic calculation using MACSYMA or MATHEMATICA.

Finally, using the polar form for the variables z_1 and z_2, $z_j=r_j\exp(-i\theta_j)$, we can convert the factor $(z_1/z_2)^{-i/k}$ in Eq. (20), which appears to be multivalued, into the following form:

$$\left[\frac{z_1}{z_2}\right]^{-i/k}=e^{-(\theta_1-\theta_2)/k}e^{-i\ln(r_1/r_2)/k} , \tag{22}$$

where

$$r_1=[1+(k+F)^2]^{1/2} , \quad r_2=[1+(k-F)^2]^{1/2} \tag{23}$$

and

$$\theta_1=\tan^{-1}(k+F) , \quad \theta_2=\tan^{-1}(F-k) \quad \text{with } -\frac{\pi}{2}\le\theta_1,\theta_2\le\frac{\pi}{2} . \tag{24}$$

The reason for choosing the principal branch for the angles θ_1 and θ_2 is that in using formulas (14), (17), (18), and (20) we need to select a single value since a hypergeometric function permits only one functional value for given arguments and variables. Furthermore, one can easily show that this branch is correct by using formula (14) or (18) with the definition of a hypergeometric function as an infinite series. Then the whole procedure can be programmed in a high-level code like FORTRAN, PASCAL, C, . . . , etc., using elementary functions for numerical calculations as well as in a batch file for a commercial mathematical package for symbolic computations. We obtain the closed expression for the transition amplitude to continuum states with quantum numbers k, l, and $m=0$ as follows:

$$C_{kl0}=(-1)^{[l/2]}i^l\left[\frac{4k}{1-e^{-2\pi/k}}\right]^{1/2} \times\frac{e^{-(\theta_1-\theta_2)/k}}{F^{l+1}r_1r_2\left[\prod_{s=0}^{l}(1+s^2k^2)\right]^{1/2}} \times[S_l(k,F)]^{1/2}\sin[\alpha_l(k,F)+\beta(k,F)] , \tag{25}$$

where θ_1, θ_2, r_1, and r_2 are defined in Eq. (24), $\beta(k,F)=k^{-1}\ln(r_1/r_2)$, $\alpha_l(k,F)=\tan^{-1}[N_l(k,F)/D_l(k,F)]$, and N_l, D_l, and S_l are polynomials of finite order in k and F which depend on l. In the Appendix, we show some of them obtained from symbolic computation using MACSYMA. From those expressions, one can easily deduce the analytic behavior of C_{kl0} in limiting cases such as $k \ll F$ and $k \gg F$, for given F or k.

III. DOUBLY DIFFERENTIAL CROSS SECTION

We now turn our attention to the angular distribution of photoelectrons and briefly review the derivation of the differential cross section (DCS) for photoionization. The result gives the correct angular distribution for a system whose wave function is known (either by direct numerical integration of the TDSE or by some other means) immediately after a finite width pulse. Assuming that the pulse terminates at time 0, denote it by $\Psi_+(\mathbf{r})=\Psi(\mathbf{r},t=0^+)$.

The relevant experimental apparatus is assumed to consist of a detector subtending the solid angle $d\Omega$ located at radius r from the interaction region, which will be taken to approach infinity. The distribution of photoelectrons is then obtained by considering the total probability that photoelectrons cross the detector after the passage of the pulse. This is given by [20]

$$d\sigma=\lim_{r\to\infty}\int_{0^+}^{\infty}dt\ \mathbf{j}(\mathbf{r},t)\cdot d\,\mathbf{A}=\lim_{r\to\infty}\int_{0^+}^{\infty}dt\ r^2 j_{\rm rad}(\mathbf{r},t)d\Omega\ , \tag{26}$$

where $j_{\rm rad}(\mathbf{r},t)$ is the radial component of the probability current evaluated at position $\mathbf{r}$ and time t. It can be expressed in terms of the wave function as

$$j_{\rm rad}(\mathbf{r},t)=\frac{1}{2i}\left[\Psi_c^*(\mathbf{r},t)\frac{\partial}{\partial r}\Psi_c(\mathbf{r},t)-\text{c.c.}\right]\ , \tag{27}$$

with $\Psi_c(\mathbf{r},t)$ taken to be only the continuum portion of the whole wave function $\Psi(\mathbf{r},t)$, which can be expanded in terms of a complete basis of Coulomb wave functions as

$$\Psi(\mathbf{r},t)=\sum_{n,l,m}C_{nlm}e^{-iE_nt}\Phi_{nlm}(\mathbf{r})+\sum_{l,m}\int_0^{\infty}dk\ C_{klm}e^{-iE_kt}\Phi_{klm}(\mathbf{r})\ . \tag{28}$$

Here one needs to pay attention to the fact that the continuum basis functions are regular solutions of the Schrödinger equation, which are standing waves rather than outgoing waves. However, it can be shown [21] that one can use the same coefficients C_{klm} in Eq. (28) in expanding $\Psi_c(\mathbf{r},t)$ in terms of outgoing waves rather than standing waves, even though the outgoing waves are irregular at the origin. Now, by expressing the basis functions in spherical polar coordinates in their asymptotic form [22] as $r\to\infty$ and performing the t integral, one of the k integrals, and one of the summations over l and m, the following expression is obtained for the DCS:

$$\frac{d\sigma}{d\Omega}=\int_0^{\infty}dk\,|f_k(\theta,\phi)|^2\ , \tag{29}$$

with

$$f_k(\theta,\phi)=\sum_{l,m}C_{klm}\,Y_{lm}(\theta,\phi)e^{i(\delta_{kl}-l\pi/2)}\ , \tag{30}$$

where δ_{kl} is the Coulomb phase given by

$$\delta_{kl}=\arg\Gamma(l+1-ik^{-1})\ . \tag{31}$$

The DDCS, defined to be the probability that the atom is photoionized with the photoelectron's momentum value lying in the range k to $k+dk$ and its direction lying in the solid angle $d\Omega$ about (θ,ϕ), is the integrand of Eq. (29):

$$\frac{d^2\sigma}{dk\,d\Omega}=|f_k(\theta,\phi)|^2\ . \tag{32}$$

These results were derived long ago by Mott and Massey [23] using a different argument.

For a linearly polarized field, the expansion coefficient C_{klm} has the form

$$C_{klm}=C_{lk0}\delta_{m,0}\ , \tag{33}$$

where $\delta_{m,0}$ is a Kronecker delta. Since $Y_{l0}=[(2l+1)/(4\pi)]^{1/2}P_l(\cos\theta)$ and $e^{-il\pi/2}=(-i)^l$, we have in this case

$$f_k(\theta,\phi)\equiv f_k(\theta)=\sum_l(-i)^l\left[\frac{2l+1}{4\pi}\right]^{1/2}C_{kl}e^{i\delta_{kl}}P_l(\cos\theta)\ . \tag{34}$$

The explicit expression for the Coulomb phase shift can be decomposed as

$$\delta_{kl}=\delta_k^{(0)}+\delta_k^{(l)}\ , \tag{35}$$

with $\delta_k^{(0)}$ independent of l since [24]

$$\arg\Gamma(l+1-ik^{-1})=\arg\Gamma(1-ik^{-1})+\sum_{n=1}^{l}\tan^{-1}\left[\frac{-1}{nk}\right]\ . \tag{36}$$

In actual evaluations of f_k, we always need to truncate the summation in Eq. (34) at a finite value of l. Denoting this maximum value of l by $l_{\rm max}$, we obtain the final expression for f_k as

$$f_k^{(l_{\rm max})}(\theta)=e^{i\delta_k^{(0)}}\sum_{l=0}^{l_{\rm max}}(-1)^l\left[\frac{2l+1}{4\pi}\right]^{1/2}C_{kl0}\times P_l(\cos\theta)\prod_{n=1}^{l}e^{i\Theta_{kn}}\ , \tag{37}$$

where

$$\Theta_{kn}=\tan^{-1}\left[\frac{-1}{nk}\right]\ . \tag{38}$$

IV. RESULTS AND DISCUSSION

In a previous paper [12], we presented photoelectron spectra for field strengths $F=0.5$, 1.0, and 2.0 a.u. including partial-wave contributions up to $l=4$ (g wave). Using the method developed in Sec. II, it is possible to evaluate the transition amplitudes to partial waves of large l rapidly, which enables us now to include partial-wave contributions of angular momentum quantum numbers up to $l_{\rm max}$ as shown in Table I to obtain the angular distributions of Fig. 1. We choose field strengths ranging from 0.05 to 5.0 a.u., and use the formula given in Eq.

(37) with the procedure in Sec. II. We can estimate the relative error involved in each curve of Fig. 1 looking at Table I. One might be misled by Table I to conclude that the perturbative regime extends to field strengths approximately around 1.0 a.u. since it shows the dominant contribution for photoionization to be the p-wave up to that field strength. That is not correct: for example, for $F=0.05$ a.u., the s- and d-wave contributions are about 10 times less than the p-wave contribution in absolute value of transition amplitude, and those of higher-l waves fall very rapidly as l increases. On the other hand, for $F=0.5$ a.u., the other partial-wave contributions become quite comparable to that of the p wave for various ranges of the photoelectron's momenta—those of the s and d waves for $k \leq 0.3$ a.u. are, respectively, about $\frac{1}{3}$ and $\frac{2}{5}$ of that of the p-wave, that of the d wave for $0.4 \leq k \leq 1.5$ a.u. is about $\frac{1}{2}$ of that of the p wave, that of the f wave for $0.5 \leq k \leq 1.0$ a.u. is about $\frac{1}{6}$ to that of the p wave, and so on. This indicates that the perturbation calculation, especially the lowest-order one, cannot be applied at this value of field strength. See also Table II.

The inapplicability of perturbation theory at high-field strengths is qualitatively evident in the polar plots of Fig. 1. The angular distribution for $F=0.05$ displays a relatively high degree of symmetry about $\theta=90°$, suggesting the dominance of the p-wave contribution, as would be expected from the lowest-order perturbation theory. For the higher values of field strength, however, the distribution of photoelectrons is localized in the direction antiparallel to the applied field, a result which is easily understood on classical grounds.

Note that the DDCS predicts, for a given polar angle, a continuous range of photoelectron momenta. Furthermore, the most probable momentum measured will, in general, also vary as the angle changes. This phenomenon, which is most evident in the polar plot for $F=1.0$, is due to the pure atomic response and is not an effect of ponderomotive scattering of the photoelectrons

TABLE I. Maximum angular quantum numbers $l_{\max}$ and absolute value of transition amplitudes $|C_{k_{\max}}|$ to be used to obtain Fig. 1 using Eqs. (25) and (37). Also shown is the maximum transition amplitude $|C_{kl}*|$ for each value of field strength F and momentum k, where l^* is the angular quantum number to give the maximum value of $|C_{kl}|$ for given F and k. The number in the square brackets indicates the exponent of basis 10.

F	k	l^*	$\lvert C_{kl}*\rvert$	$l_{\max}$	$\lvert C_{kl_{\max}}\rvert$	F	k	l^*	$\lvert C_{kl}*\rvert$	$l_{\max}$	$\lvert C_{kl_{\max}}\rvert$
	0.01	1	0.006 246 566	4	1.27[−7]		0.01	1	0.056 817 831	7	3.07[−7]
	0.05	1	0.013 906 714	4	3.08[−7]		0.05	1	0.126 674 607	7	7.54[−7]
	0.1	1	0.019 400 951	4	4.35[−7]		0.1	1	0.177 502 408	7	1.664[−6]
	0.3	1	0.029 219 018	4	1.206[−6]		0.3	1	0.278 728 974	8	3.076[−6]
0.05	0.4	1	0.030 079 851	4	1.580[−6]	0.5	0.5	1	0.296 669 593	10	1.056[−6]
	0.5	1	0.029 278 098	4	1.863[−6]		0.7	1	0.266 381 708	11	8.36[−7]
	0.7	1	0.024 931 825	4	1.948[−6]		1.0	1	0.189 582 762	11	8.51[−7]
	1.0	1	0.017 010 391	4	1.344[−6]		1.5	1	0.090 104 564	11	3.07[−7]
	2.0	1	0.003 951 453	4	1.76[−7]		2.0	1	0.043 026 235	10	2.51[−7]
	0.01	1	0.068 853 320	7	1.086[−6]		0.1	0	0.083 781 897	7	4.35[−7]
	0.05	1	0.153 891 646	7	2.821[−6]		0.5	0	0.188 549 989	10	1.164[−6]
	0.1	1	0.217 323 717	8	1.036[−6]		1.0	1	0.324 968 10	13	2.268[−5]
	0.3	1	0.369 621 357	9	3.259[−6]		1.3	1	0.410 125 22	17	4.901[−5]
	0.5	1	0.453 599 126	11	2.298[−6]		1.5	1	0.449 241 8	18	1.353[−4]
1.0	0.7	1	0.483 515 065	13	6.041[−6]	2.0	1.7	1	0.459 111 3	20	1.491[−4]
	1.0	1	0.431 729 556	15	4.471[−6]		2.0	2	0.411 811 2	22	1.851[−4]
	1.5	1	0.238 378 334	16	5.463[−6]		2.3	2	0.315 481 3	23	1.036[−4]
	2.0	1	0.110 924 828	15	2.581[−6]		2.5	2	0.242 361 92	24	3.959[−5]
	2.5	1	0.054 028 595	14	6.13[−7]		3.0	2	0.112 274 910	23	8.044[−6]
	3.0	1	0.028 726 969	13	1.68[−7]		4.0	1	0.030 402 802	19	4.96[−7]
	0.5	0	0.074 696 576	8	5.29[−7]		1.0	0	0.021 125 392	8	4.50[−7]
	1.0	0	0.112 699 409	12	2.588[−6]		2.0	0	0.036 013 825	12	4.343[−6]
	1.5	1	0.159 575 90	14	1.807[−5]		3.0	1	0.068 234 59	18	4.458[−5]
	2.0	1	0.256 844 45	18	7.257[−5]		4.0	2	0.171 353 8	26	4.110[−4]
	2.5	2	0.356 360 1	24	4.484[−4]		4.5	3	0.267 259 8	35	6.252[−4]
3.0	3.0	2	0.373 325 7	29	3.890[−4]	5.0	5.0	4	0.301 875 8	45	7.028[−4]
	3.5	2	0.229 167 61	31	8.490[−5]		5.5	4	0.199 285 5	41	6.953[−4]
	4.0	2	0.111 799 46	30	1.628[−5]		6.0	3	0.100 874 6	38	1.322[−4]
	4.5	2	0.055 363 842	26	5.963[−6]		7.0	2	0.028 320 809	33	3.400[−6]
	5.0	2	0.029 544 016	24	1.039[−6]		8.0	2	0.010 936 445	28	5.15[−7]
	6.0	1	0.011 312 806	20	2.46[−7]		10.0	1	0.002 864 101	19	1.50[−7]

inasmuch as the latter is a result only of the spatial intensity gradients of temporally finite laser pulses.

With realistic, finite-width pulses one expects more complicated behavior such as the appearance of multiple uniformly spaced peaks in the photoelectron spectra, the well-known ATI structure, but even then our calculation presented here (viz., the behavior of the photoelectron spectra with respect to varying intensity) can be of use in analyzing the situation. For example, we have carried out calculations of the magnitude of transition amplitudes to partial-wave states with a wide range of photoelectron momenta for field strengths up to 10 a.u. From this one can predict possible channels of significant contribution to photoionization for given laser parameters. Specifically, for the case $F=k=5$ a.u., the magnitudes of transition amplitudes are of the order of 10^{-1}, 10^{-2}, and 10^{-3} for the range of angular quantum numbers $0\le l\le 15$, $16\le l\le 29$, and $30\le l\le 43$, respectively,

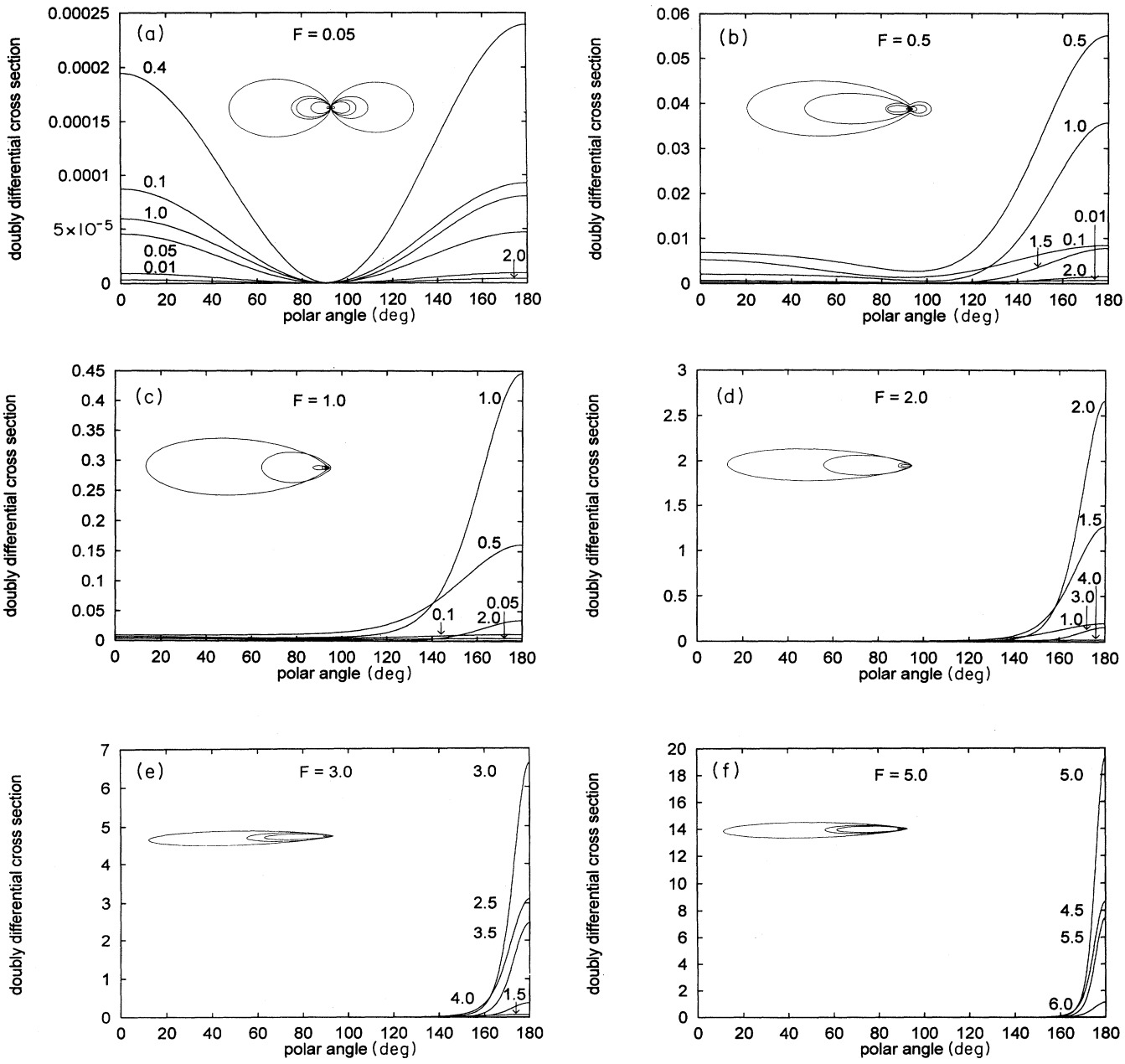

FIG. 1. Angular distributions of photoelectrons for various field strengths $F=0.05$, 0.5, 1.0, 2.0, 3.0, and 5.0 a.u. The momentum value is indicated on each curve, and also shown inside each graph are the polar plots. Refer to Table I to see numerical convergence and error involved in drawing each curve.

whereas for $k=4$ a.u., these magnitudes correspond to $0, \leq l \leq 6$, $7 \leq l \leq 15$, and $16 \leq l \leq 24$, respectively. Therefore, one can deduce that at this field strength the number of accessible channels for a given order of probability approximately doubles as the photoelectron momentum increases from 4 to 5 a.u., which is true as long as the dipole approximation is valid.

In summary, the method presented herein enables one to reduce an expression involving hypergeometric functions, which may obscure the physical behavior and induce large computational times, to a closed form in terms of elementary functions. This technique, which is quite

TABLE II. Differential cross section integrated over some range of polar angles. The same l_{max} is used to obtain the numerical value for each F and k_0 as is given in Table I.

		Polar-angle rangle for integration						Polar-angle rangle for integration			
F	k_0	0°–180°[a]	0°–90°[b]	150°–180°[c]	170°–180°[d]	F	k_0	0°–180°[a]	0°–90°[b]	150°–180°[c]	170°–180°[d]
	0.01	0.000 039	49.9	17.5	2.24		0.01	0.003 988	49.4	13.2	1.65
	0.04	0.000 156	49.7	17.6	2.26		0.1	0.039 047	44.1	15.9	2.03
	0.08	0.000 306	49.4	17.8	2.29		0.2	0.073 204	38.5	19.4	2.55
	0.16	0.000 571	48.8	18.2	2.34		0.3	0.098 471	33.5	23.3	3.13
	0.32	0.000 877	47.8	18.8	2.43		0.4	0.112 536	29.3	27.2	3.77
0.05	0.64	0.000 703	46.6	19.7	2.56	0.5	0.5	0.115 238	25.9	31.1	4.42
	1.28	0.000127	46.4	19.9	2.58		0.6	0.108 446	23.3	34.6	5.05
	2.56	0.000 004	47.5	19.2	2.48		0.8	0.079 282	20.2	40.2	6.09
							1.1	0.036 495	18.7	44.3	6.87
							1.4	0.014 345	19.4	44.7	6.91
							2.0	0.002 231	22.8	41.2	6.18
	0.01	0.006 441	49.3	11.4	1.40		0.05	0.036 082	46.3	10.8	1.31
	0.05	0.032 115	46.5	12.6	1.56		0.2	0.143 721	35.5	15.9	1.52
	0.1	0.063 667	43.0	14.2	1.79		0.4	0.280 027	23.5	25.0	3.44
	0.2	0.122 821	36.4	18.0	2.34		0.6	0.385 993	15.2	36.2	5.48
	0.3	0.172 954	30.5	22.3	3.00		0.7	0.415 640	12.3	42.0	6.71
	0.4	0.209 879	25.5	27.1	3.78		0.8	0.423 762	10.1	47.5	8.01
	0.5	0.230 478	21.4	32.0	4.63		0.9	0.408 911	8.53	52.6	9.33
0.7	0.6	0.233 660	18.3	36.8	5.55	1.0	1.0	0.373 537	7.41	57.1	10.6
	0.7	0.221 007	15.9	41.3	6.45		1.1	0.323 678	6.65	60.8	11.7
	0.8	0.196 540	14.2	45.3	7.29		1.3	0.211438	5.90	65.8	13.3
	1.0	0.133 243	12.3	51.1	8.62		1.5	0.120 297	5.85	68.2	14.0
	1.3	0.057 475	11.8	55.0	9.49		1.7	0.063 401	6.26	68.6	13.9
	1.6	0.021 814	12.7	54.9	9.35		2.1	0.016 788	7.89	66.1	12.8
	1.9	0.008 274	14.4	52.9	8.77		2.5	0.004 827	10.1	61.8	11.2
	2.5	0.001 419	18.4	47.4	7.45		3.1	0.000 949	13.8	55.1	9.29
	0.1	0.037 107	43.1	10.4	1.25		0.1	0.012 847	44.0	9.37	1.11
	0.2	0.075 572	36.5	13.2	1.63		0.2	0.026 222	38.2	11.6	1.39
	0.4	0.161 862	24.7	20.6	2.71		0.4	0.056 833	27.5	17.3	2.19
	0.6	0.267 990	15.7	30.5	4.39		0.6	0.097 123	18.7	24.9	3.38
	0.8	0.396 021	9.60	42.3	6.84		0.8	0.154 119	12.0	34.5	5.14
	1.0	0.528 717	5.85	54.7	10.1		1.0	0.236 761	7.41	45.7	7.67
	1.2	0.617 874	3.74	65.7	14.1		1.2	0.353 234	4.45	57.6	11.1
	1.4	0.604 122	2.64	74.1	18.0		1.4	0.500 920	2.68	68.7	15.6
1.5	1.6	0.480 582	2.14	79.6	21.1	2.0	1.6	0.646 902	1.68	77.9	20.9
	1.8	0.315 169	2.00	82.5	22.8		1.8	0.719 245	1.14	84.4	26.2
	2.0	0.179 264	2.10	83.6	23.2		2.0	0.655 693	0.89	88.5	30.5
	2.2	0.094 138	2.39	83.5	22.5		2.2	0.483 566	0.81	90.7	33.0
	2.4	0.048 064	2.82	82.4	21.3		2.4	0.298 188	0.84	91.6	33.6
	2.8	0.012 972	4.06	78.7	18.4		2.6	0.163 461	0.96	91.5	32.7
	3.2	0.003 959	5.64	74.0	15.7		2.8	0.084 665	1.17	91.0	30.9
	3.6	0.001 778	6.97	70.3	14.1		3.2	0.022 499	1.82	88.4	26.4
							3.6	0.006 640	2.75	84.7	22.3
							4.0	0.002 247	3.91	80.3	19.1

[a]Actual value.

[b–d]Percentage of the value in the first column.

general, allows the evaluation of accurate, highly converged values of transition amplitudes and angular distributions for photoelectrons generated by a δ-function pulse, a calculation which would have been prohibitively lengthy via numerical computations using hypergeometric functions directly.

ACKNOWLEDGMENT

It is our pleasure to express thanks to Sun Microsystems, Inc., for the gift of a SPARCstation 1+, under their Academic Grants Program, which has been used for the present computations.

APPENDIX: POLYNOMIALS N_l, D_l, S_l FOR $l=0,1,2,3$

$$D_0(k,F)=-2(k^2-F^2+1)\ ,$$

$$N_0(k,F)=4F\ ,$$

$$S_0(k,F)=4(k^2-2kF+F^2+1)(k^2+2kF+F^2+1)\ ,$$

$$D_1(k,F)=2\sqrt{3}(k^2+1)(k^2-F^2+1)\ ,$$

$$N_1(k,F)=-4\sqrt{3}F(k^2+1)\ ,$$

$$S_1(k,F)=12(k^2+1)^2(k^2-2kF+F^2+1)(k^2+2kF+F^2+1)\ ,$$

$$D_2(k,F)=\frac{\sqrt{5}}{2}(9k^6-7k^4F^2+27k^4-5k^2F^4-2k^2F^2+27k^2+3F^6+7F^4+5F^2+9)\ ,$$

$$N_2(k,F)=-\sqrt{5}F(9k^4-4k^2F^2+18k^2+3F^4+8F^2+9)\ ,$$

$$\begin{aligned}S_2(k,F)=&\tfrac{5}{4}(k^2-2kF+F^2+1)(k^2+2kF+F^2+1)\\&\times(81k^8+36k^6F^2+324k^6-50k^4F^4+324k^4F^2+486k^4-12k^2F^6-52k^2F^4+540k^2F^2\\&+324k^2+9F^8+60F^6+142F^4+252F^2+81)\ ,\end{aligned}$$

$$\begin{aligned}D_3(k,F)=&-\frac{\sqrt{7}}{2}(30k^8-21k^6F^2+120k^6-9k^4F^4+9k^4F^2+180k^4-15k^2F^6+50k^2F^4\\&+81k^2F^2+120k^2+15F^8+45F^6+59F^4+51F^2+30)\ ,\end{aligned}$$

$$N_3(k,F)=\sqrt{7}F(30k^6-11k^4F^2+90k^4-10k^2F^4+50k^2F^2+90k^2+15F^6+50F^4+61F^2+30)\ ,$$

$$\begin{aligned}S_3(k,F)=&\tfrac{7}{4}(k^2-2kF+F^2+1)(k^2+2kF+F^2+1)\\&\times(900k^{12}+540k^{10}F^2+5400k^{10}+81k^8F^4+7020k^8F^2+13\,500k^8-900k^6F^6+5220k^6F^4\\&+22\,680k^6F^2+18\,000k^6-270k^4F^8-20k^4F^6+20\,358k^4F^4+31\,320k^4F^2+13\,500k^4\\&+2100k^2F^8+11\,300k^2F^6+25\,380k^2F^4+19\,980k^2F^2+5400k^2+225F^{12}+1800F^{10}\\&+5970F^8+10\,420F^6+10\,161F^4+4860F^2+900)\ .\end{aligned}$$

[1] P. Agostini, F. Fabre, G. Mainfray, G. Petite, and N. K. Rahman, Phys. Rev. Lett. **42**, 1127 (1979).

[2] P. Kruit, J. Kimman, H. G. Muller, and M. J. van der Wiel, Phys. Rev. A **28**, 248 (1983); L. A. Lompré, A. L'Huillier, G. Mainfray, and C. Manus, J. Opt. Soc. Am. B **2**, 1906 (1985); P. H. Bucksbaum, M. Bashkansky, R. R. Freeman, T. J. McIlrath, and L. F. Dimauro, Phys. Rev. Lett. **56**, 2590 (1986); U. Johann, T. S. Luk, H. Egger, and C. K. Rhodes, Phys. Rev. A **34**, 1084 (1986).

[3] J. Kupersztych, Eur. Phys. Lett. **4**, 23 (1987); W. Xiong, F. Yergeau, and S. L. Chin, in *Proceedings of the International Conference on Multiphoton Processes IV,* edited by S. J. Smith and P. L. Knight (Cambridge University Press, Cambridge, England, 1988); S.-I. Chu and R. Y. Yin, J. Opt. Soc. Am. B **4**, 720 (1988).

[4] R. R. Freeman, P. H. Bucksbaum, H. Milchberg, S. Darack, D. Schumacher, and M. E. Geusic, Phys. Rev. Lett. **59**, 1092 (1987); P. Agostini, P. Breger, A. L'Huillier, H. G. Muller, G. Petite, A. Antonetti, and A. Migus, *ibid.* **63**, 2208 (1989); **64**, 815 (1990); H. Rottke, B. Wolff, M. Brickwedde, D. Feldmann, and K. H. Welge, *ibid.* **64**, 404 (1990).

[5] J. H. Eberly and J. Javanainen, Phys. Rev. Lett. **60**, 1346 (1988); T. J. McIlrath, R. R. Freeman, W. E. Cooke, and L. D. van Woerkom, Phys. Rev. A **40**, 2770 (1989); Y. Gontier and M. Trahin, *ibid.* **46**, 1488 (1992); M. Dörr, D. Feldmann, R. M. Potvliege, H. Rottke, R. Shakeshaft, K. H. Welge, and B. Wolff-Rottke, J. Phys. B **25**, L275 (1992).

[6] M. Ferray, A. L'Huillier, X. F. Li, L. A. Lompré, G. Mainfray, and C. Manus, J. Phys. B **21**, L31 (1988); M. D. Perry, A. Szöke, and K. C. Kulander, Phys. Rev. Lett. **63**,

1058 (1989); L. A. Lompré, A. L'Huillier, M. Ferray, P. Monot, G. Mainfray, and C. Manus, J. Opt. Soc. Am. B **7**, 754 (1990); N. Sarukura, K. Hata, T. Adachi, R. Nodomi, M. Watanabe, and S. Watanabe, Phys. Rev. A **43**, 1669 (1991).

[7] J. H. Eberly, Q. Su, and J. Javanainen, Phys. Rev. Lett. **62**, 881 (1989); R. M. Potvliege and R. Shakeshaft, Phys. Rev. A **40**, 3061 (1989); A. L'Huillier, K. J. Schafer, and K. C. Kulander, Phys. Rev. Lett. **66**, 2200 (1991); J. L. Krause, K. J. Schafer, and K. C. Kulander, Phys. Rev. A **45**, 4998 (1992); G. D. Billing, N. E. Henriksen, and C. Leforestier, *ibid.* **45**, R4229 (1992).

[8] R. R. Jones and P. H. Bucksbaum, Phys. Rev. Lett. **67**, 3215 (1991), and references therein.

[9] M. Pont, N. R. Walet, M. Gavrila, and C. W. McCurdy, Phys. Rev. Lett. **61**, 939 (1988); M. Dörr, R. M. Potvliege, and R. Shakeshaft, *ibid.* **64**, 2003 (1990); Q. Su and J. H. Eberly, Phys. Rev. A **43**, 2474 (1991); R. Grobe and M. V. Fedorov, Phys. Rev. Lett. **68**, 2592 (1992).

[10] See, e.g., J. Grochmalicki, M. Lewenstein, and K. Rzążewski, Phys. Rev. Lett. **66**, 1038 (1991); T. Ménis, R. Taïeb, V. Véniard, and A. Maquet, J. Phys. B **25**, L263 (1992).

[11] H. A. Kramers, *Collected Scientific Papers* (North-Holland, Amsterdam, 1956), p. 866; W. C. Henneberger, Phys. Rev. Lett. **21**, 838 (1968). For applications to stabilization against ionization, see, e.g., Q. Su, J. H. Eberly, and J. Javanainen, Phys. Rev. Lett. **64**, 862 (1990); R. Grobe and C. K. Law, Phys. Rev. A **44**, 4114 (1991); M. Horbatsch, Phys. Lett. A **165**, 58 (1992).

[12] M. D. Girardeau, K. G. Kim, and C. C. Widmayer, Phys. Rev. A **46**, 5932 (1992).

[13] B. Wolff, H. Rottke, D. Feldmann, and K. H. Welge, Z. Phys. D **10**, 35 (1988); H. Bachau, P. Lambropoulos, and X. Tang, Phys. Rev. A **42**, 5801 (1990); D. Kim, S. Fournier, M. Saeed, and L. F. Dimauro, *ibid.* **41**, 4966 (1990).

[14] H. G. Muller, G. Petite, and P. Agostini, Phys. Rev. Lett. **61**, 2507 (1988); K. J. Schafer and K. C. Kulander, Phys. Rev. A **42**, 5794 (1990); R. M. Potvliege and R. Shakeshaft, *ibid.* **41**, 1609 (1990); D. S. Guo and G. W. F. Drake, *ibid.* **45**, 6622 (1992).

[15] M. Trippenbach, K. Rzążewski, M. V. Fedorov, and A. E. Kazakov, J. Phys. B **22**, 1193 (1989); P. N. Price and D. A. Harmin, Phys. Rev. A **42**, 2555 (1990); S. D. Oh and R. H. Pratt, *ibid.* **45**, 1583 (1992).

[16] H. A. Bethe and E. E. Salpeter, *Quantum Mechanics of One- and Two-Electron Atoms* (Plenum, New York, 1977), pp. 21–25.

[17] The confluent hypergeometric function is a well-convergent series for values of its arguments and variable relevant to the hydrogenic wave function.

[18] Refer to, e.g., I. S. Gradshteyn and I. M. Ryzhik, *Table of Integrals, Series, and Products* (Academic, New York, 1980).

[19] A. Erdélyi, W. Magnus, F. Oberhettinger, and F. G. Tricomi, *Higher Transcendental Functions* (McGraw-Hill, New York, 1953), Vol. I, pp. 101–105.

[20] For the sake of mathematical convenience, we take the position of the detector to be at infinity. But the limit $r \to \infty$ in this expression should be taken after the time integral since the detector performing the time integration is actually placed at a large but finite distance, i.e., $a_0 \ll r < \infty$.

[21] M. D. Girardeau (unpublished).

[22] The asymptotic expression for the continuum wave function on p. 22 of Ref. [16] has the wrong sign in front of the Coulomb phase factor. The proper expression for outgoing wave is, for its radial part, $R_{kl}^{\rm out}(r) \sim \pi^{-1/2} r^{-1} \exp\{i[kr + k^{-1}\ln(2kr) - l\pi/2 + \delta_{kl}]\}$.

[23] N. F. Mott and H. S. W. Massey, *The Theory of Atomic Collisions,* 2nd ed. (Clarendon, Oxford, 1949), pp. 353–356.

[24] *Handbook of Mathematical Functions,* edited by M. Abramowitz and I. A. Stegun (U.S. GPO, Washington, DC, 1964), Eq. 6.1.24, p. 256.